

Active Suppression of Acoustically Induced Jitter for the Airborne Laser

Roger M. Glaese,^{*} Eric H. Anderson, and Paul C. Janzen
CSA Engineering, Inc., 2565 Leghorn Street, Mountain View, CA 94043

ABSTRACT

The Airborne Laser (ABL) system has extremely tight jitter requirements. Acoustic disturbances, such as those caused by the pressure recovery system of the high power laser, are a significant jitter source. Several technologies may be appropriate for reducing the acoustically induced jitter. The first choice for mitigation will be passive approaches, such as acoustic blankets. There is, however, some uncertainty whether these approaches will provide sufficient attenuation and there is concern about the weight of these approaches. A testbed that captured the fundamental physics of the ABL acoustically induced optical jitter problem was developed. This testbed consists of a flexure-mounted mirror exposed to an acoustic field that is generated outside a beam tube and then propagates within the tube. Both feedback and adaptive feedforward control topologies were implemented on the testbed using either of two actuators (a fast steering mirror and a secondary acoustic speaker located near the precision mirror), and a variety of sensors (microphones measuring the acoustic disturbance, accelerometers and microphones mounted on the precision optic, and an optical position sensing detector). This paper summarizes the results from these control topologies for reducing the acoustically induced jitter with some control topologies achieving in excess of 40 dB jitter reduction at a single frequency. This work was performed under an SBIR Phase I funded by the Air Force Research Laboratory Space Vehicles Directorate (AFRL/VS).

Keywords: Active noise control, Airborne Laser, Feedforward control, Jitter, Precision optics

1. INTRODUCTION

The Airborne Laser, shown in Figure 1, is a weapon system designed to destroy ballistic missiles by delivering lethal levels of thermal energy. The use of directed energy systems requires precision in both tracking the target and pointing the weapon at the target. This precision must be maintained over sustained periods of time as the effect of the weapon is thermal—the energy beam must be focused on a fixed region of the target long enough to deliver the amount of energy necessary to destabilize the target. Historically, the greatest challenge to maintaining the required precision is controlling the inertial motion of the optics that direct the beam. Mechanical motion of the steering and shaping optics induce jitter—the dynamic deviation of the beam from an inertially stable trajectory through space. An airborne platform is by design compliant—it is not the type of stiff, stable platform required for a precision optical system. Fortunately, Team ABL is not building the first airborne laser system. That distinction goes to the Airborne Laser Laboratory (ALL). ALL was designed and built to demonstrate that microradian-precision pointing and tracking could be obtained in an airborne operational laboratory. The results of ALL testing revealed several important lessons learned concerning jitter and its mitigation. Foremost among these were the degrading effects of acoustically induced jitter. Active acoustic control has the potential to increase the effectiveness of the ABL system.



Figure 1: YAL-1 Airborne Laser system

^{*} Correspondence: Email: roger.glaese@csaengineering.com; www.csaengineering.com; Telephone (650) 210-9000; Fax: (650) 210-9001

Report Documentation Page				Form Approved OMB No. 0704-0188	
Public reporting burden for the collection of information is estimated to average 1 hour per response, including the time for reviewing instructions, searching existing data sources, gathering and maintaining the data needed, and completing and reviewing the collection of information. Send comments regarding this burden estimate or any other aspect of this collection of information, including suggestions for reducing this burden, to Washington Headquarters Services, Directorate for Information Operations and Reports, 1215 Jefferson Davis Highway, Suite 1204, Arlington VA 22202-4302. Respondents should be aware that notwithstanding any other provision of law, no person shall be subject to a penalty for failing to comply with a collection of information if it does not display a currently valid OMB control number.					
1. REPORT DATE 2000		2. REPORT TYPE		3. DATES COVERED 00-00-2000 to 00-00-2000	
4. TITLE AND SUBTITLE Active Suppression of Acoustically Induced Jitter for the Airborne Laser				5a. CONTRACT NUMBER	
				5b. GRANT NUMBER	
				5c. PROGRAM ELEMENT NUMBER	
6. AUTHOR(S)				5d. PROJECT NUMBER	
				5e. TASK NUMBER	
				5f. WORK UNIT NUMBER	
7. PERFORMING ORGANIZATION NAME(S) AND ADDRESS(ES) CSA Engineering,2565 Leghorn Street,Mountain View,CA,94043				8. PERFORMING ORGANIZATION REPORT NUMBER	
9. SPONSORING/MONITORING AGENCY NAME(S) AND ADDRESS(ES)				10. SPONSOR/MONITOR'S ACRONYM(S)	
				11. SPONSOR/MONITOR'S REPORT NUMBER(S)	
12. DISTRIBUTION/AVAILABILITY STATEMENT Approved for public release; distribution unlimited					
13. SUPPLEMENTARY NOTES The original document contains color images.					
14. ABSTRACT see report					
15. SUBJECT TERMS					
16. SECURITY CLASSIFICATION OF:			17. LIMITATION OF ABSTRACT	18. NUMBER OF PAGES 14	19a. NAME OF RESPONSIBLE PERSON
a. REPORT unclassified	b. ABSTRACT unclassified	c. THIS PAGE unclassified			

An additional difficulty faced in the ABL is an acoustic environment inside the aircraft even more severe than the ALL, especially during operation of the high power laser devices. This acoustic field causes increased optical jitter. The extent of the acoustic jitter problem will be quantified by performing structural-acoustic analysis of the subassemblies of the optical train. One approach for mitigating this acoustic jitter is to mount passive acoustic blankets in the aircraft in an effort to reduce the overall sound levels. Typically, though, passive blankets are limited in their effectiveness at low frequencies, with a two to four inch thick passive blanket effective only down to 300 to 500 Hz. Blankets can be made more effective at lower frequencies only by increasing their thickness, which also adds significantly to their mass. Additionally, blankets typically only reduce the overall acoustic field by approximately a factor of two. It is expected that the desired levels of jitter reduction will require at least an order of magnitude reduction in the acoustic field in the vicinity of a relatively few optical components and subassemblies. Because of these properties of passive blankets and the high levels of acoustic suppression required at the optical elements, there is considerable uncertainty whether passive blankets alone will be able to meet the acoustic performance objectives. Active solutions, however, are attractive for the acoustic problem because they can achieve the needed large reduction in a local spatial region with good weight efficiency.

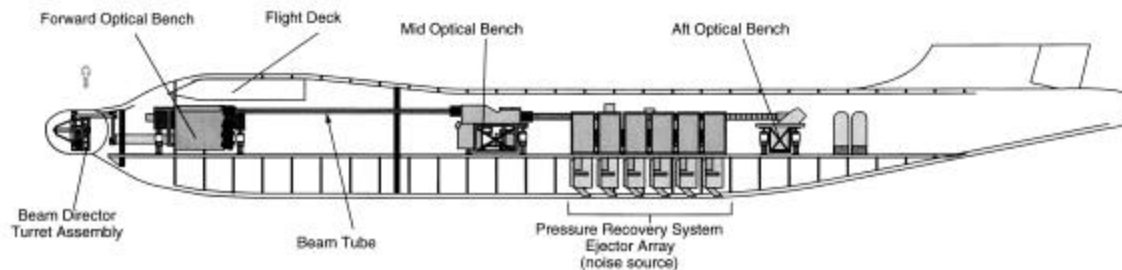


Figure 2: Schematic of ABL aircraft and optical train

1.1 Acoustically Induced Optical Jitter

Figure 2 shows a schematic of the ABL aircraft and the major subassemblies of the optical train. Jitter in the ABL optical train increases the length of time that the beam must be held on the target in order to destroy it. The current total ABL jitter budget is less than a microradian. Sensor noise accounts for a substantial fraction of the jitter budget and cannot realistically be reduced very much. The remaining budget is allotted to mechanical and acoustic vibrations, representing a serious challenge to the state of the art. Because of this tight jitter requirement, a significant investment is being made in active mechanical vibration isolation of the major components and subassemblies of the optical train. The acoustic contribution, on the other hand, is less well understood at this point.

The dominant sources of acoustic disturbances are the pressure recovery system (PRS) of the COIL laser and the unsteady aerodynamic pressures that impinge on the turret. The acoustic noise in the aft end of the plane arises from a high pressure jet that exhausts into the atmosphere from ejector tubes in the lower rear portion of the aircraft fuselage. Perhaps the most challenging acoustic problems arise in the turret, where external unsteady aerodynamic flow fields generate high amplitude acoustic fields that impinge directly on the large optical surfaces within the turret. These external flow fields generate dynamic loads on the turret that are difficult to predict. The spatial and temporal characteristics of these flow fields are complex functions of boundary layer thickness, convection velocity, geometry, and Mach number. These fields are physically distinct and are characterized as by products of attached flow, unattached flow, modified attached flow, and shock zone. This complexity makes analytical predictions of the internal fields extremely difficult and susceptible to erroneous results.

Since the dominant sources of the acoustic disturbances are well known, one possible solution might be to mechanically and acoustically isolate the optics from the rest of the aircraft. This is not really a viable option due to volume and weight constraints. In considering the use of passive blankets to attenuate some of the sound generated by the PRS ejectors, it is noted that the spectrum rolls off above 300 Hz. Thus, since the effectiveness of conventional blankets is limited in this frequency range, very thick blankets would be required to achieve significant attenuation of the PRS acoustic excitation. This is also true for the turret where volume constraints and stray light preclude the use of acoustic blankets entirely.

The uncertainty about the effectiveness of the passive acoustic mitigation approaches drives one to consider active approaches. Active approaches are attractive in that high performance levels can be achieved in local regions with good efficiency. There is a wide range of potential active acoustic suppression approaches available for ABL. The question, then,

becomes how to choose those most appropriate for the ABL case. The general criteria that an approach must satisfy are modularity, non-intrusiveness, and autonomy. Modularity means that the approach must rely on a standardized set of hardware and software that can be rapidly swapped in and out of the optical train. The second criterion refers to the fact that those responsible for the subassembly will reject an approach that necessitates a major subassembly redesign or is too risky. The final criterion, autonomy, refers to the need to be able to install the approach and have it function with minimal hands-on adjustment, since access to the ABL during flight will be severely restricted.

This paper summarizes work that was performed under an SBIR Phase I funded by the Air Force Research Laboratory Space Vehicles Directorate (AFRL/VS).

2. JITTER SUPPRESSION APPROACHES

The active jitter suppression techniques studied in this effort can be broadly classified in two categories depending on the actuator used to control the jitter, active noise control using secondary acoustic sources and active optical control using a fast steering mirror. Both of these categories have potential application to ABL optical components. As an example of active noise control using a secondary acoustic source, consider the feedforward of a microphone measuring the incoming acoustic disturbance to a small speaker located near an optical element. The intent is to try to cancel the acoustic field as measured by a performance microphone near the optical component. The mechanism for control of the jitter is the reduction in the acoustic field near the vibrating mirror. By reducing the acoustic field near the mirror, the disturbance on the mirror and the subsequent vibration are reduced and the jitter is alleviated. By using an independent actuator, the interaction with other control systems, which can potentially lead to instability, is minimized. In the second control topology, the actuator is an optical actuator (fast steering mirror), which provides direct control over the jitter. In this topology, a measure of the acoustically induced jitter, such as a microphone measurement or accelerometer measurement on the optic, is used to derive control commands to reduce the jitter, as measured by an optical sensor. It is expected that this second topology should yield the best results, since the jitter is being controlled directly. A desirable feature of the jitter suppression techniques is that they be adaptive. This is because the acoustic disturbances seen by the optical element change quite dramatically with the laser devices operating and with them off. If the control is operating continuously, it must be able to handle these abrupt changes and still function well. If the control is only operational during laser firing, the implications of startup transients on the performance must be understood.

3. HARDWARE DEMONSTRATION

The approach taken in this research was to explore candidate acoustic jitter suppression approaches by performing tests on representative hardware. This section describes that hardware, gives background on the different algorithms and architectures, and summarizes test results.

3.1 Testbed

A testbed to demonstrate active control of acoustically induced jitter was designed and built. The testbed, shown in schematic in the left hand figure and in a photograph in the right hand figure of Figure 3, consists of a length of tube of the same diameter as the real ABL laser tube with an elbow in it. One length of the tube is long (approximately 7 feet) and the other length is short (approximately 2 feet). The reason for the long length of beam tube is to insure that the axial acoustic modes of the tube are reasonably low in frequency. Ideally, one would want the length of tube that would be the same length as the ABL duct, but the hundred or so feet of length for the real tube would not fit in a laboratory setting. Both ends of the beam tube that are open to the laboratory are terminated with plywood end caps. Design of the beam tube simulator was complicated by the fact that the design for the ABL beam tube had not been finalized. A composite material was chosen for the tube simulator because of the superior strength-to-weight ratio and the cost relative to plastic or metal materials. The acoustic chamber is a heavy wood structure enclosing the beam tube simulator. The purpose of the acoustic chamber is to contain most of the acoustic energy inside the chamber and to direct it into the beam tube simulator down which it will propagate to impinge on the mirror. The acoustic chamber is suspended from the ceiling above the optical bench.

A flexure-mounted turning flat that is exposed to the acoustic field is mounted at the elbow, as shown in the upper left photograph of Figure 4. The acoustic enclosure for the optical bench assembly is similar in construction to the acoustic enclosure for the beam tube simulator, with the addition of a lexan window so that the optics can be seen from outside the testbed. The primary purpose of this acoustic enclosure is to keep as much of the acoustic disturbance as possible inside the testbed enclosure while preventing extraneous acoustic disturbances from entering the testbed. Acoustic disturbances enter the beam tube from two directions, through the wall and propagating along the duct. To make sure that the disturbances enter from upstream of the mirror, a reverberant box containing several speakers was built around the beam tube to simulate the aircraft reverberant enclosure. To simulate disturbances that emanate from well upstream of the optic and are essentially

plane waves, a speaker array was mounted at the end of the long section of tube. Both of these disturbance sources are seen in the photograph in the upper right photograph of Figure 4.

The optical bench assembly includes the actual bench hardware, the mounting hardware for the optics, and the acoustic enclosure for the optics. The optical bench consists of a Newport 3 foot by 5 foot breadboard tabletop sitting on a standard set of legs. The legs are active isolation mounts in which the passive and active isolation stages have been shorted. The optics mounting hardware consists of several stiff-backs. The stiff-back consists of vertical and horizontal plates reinforced with two triangular plates, all made of 1.5 inch thick aluminum or steel. Several of these stiff-backs were used to mount the optics at the required locations on the breadboard and in the proper orientation.

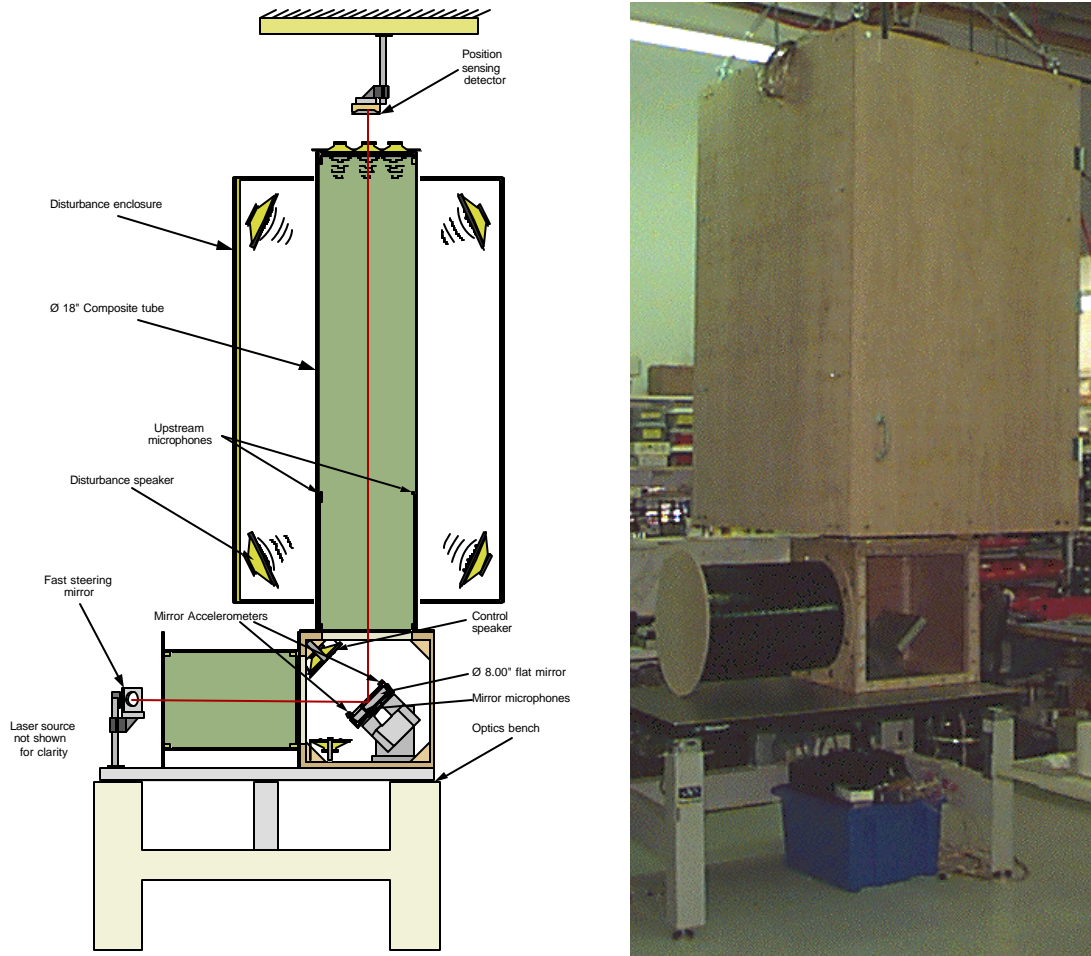


Figure 3: ABL acoustic jitter suppression testbed

Disturbance measurement microphones were distributed along the length of the long tube, both inside and outside the tube. Performance/feedback sensors, in the form of accelerometers and microphones, were also placed on or near the turning flat. Control speakers were also included in the optical enclosure. A laser metrology system was also included in the testbed. This metrology system consists of a laser mounted on the optics breadboard at the start of the short beam tube that shines a beam on a Burleigh fast steering mirror (FSM), shown in the lower photograph of Figure 4, that then enters the beam tube through a small hole, reflects off of the turning flat and propagates up into and through long beam tube. The beam then exits the long beam tube through another small hole and shines on an On-Trak Photonics model OT-3210 photodiode position sensing detector (PSD), which provides a measure of the acoustically induced jitter. The position sensing detector was mounted to the ceiling beam from which the acoustic enclosure was also hung. The Burleigh piezoelectric FSM was used as a structural actuator to cancel the acoustically induced jitter as measured by either the laser metrology system, accelerometers on the turning flat, or microphones near the turning flat. The Burleigh FSM and large diameter mirror were loaned by Lockheed Martin.

The first concern was whether the acoustics would cause enough jitter to be measured. Figure 5 shows a comparison of the ambient power spectral densities for two axes of the position sensing detector and the same power spectral density when the acoustic disturbance is on. In this case, the acoustic disturbance levels inside the disturbance enclosure was in excess of 100 dB, resulting in approximately 85 dB sound levels in the optics enclosure. Note that the power spectral density with the disturbance on is several orders of magnitude larger than the ambient power spectral density, indicating that there is measurable acoustically induced jitter. To put the plots in perspective, the ambient and disturbed position sensing detector voltages in the upper plot correspond to angular jitter levels of 6.9 and 149.3 microradians rms, respectively, and for the lower plot, 3.7 and 115.9 microradians rms, respectively. For future reference, a 1 volt output of the position sensing detector is equivalent to 378.6 microradians of angular displacement.



Figure 4: Closeup photographs of various elements of the ABL acoustic jitter suppression testbed

The control topologies were divided into two categories: feedforward and feedback. Feedforward controllers were implemented using variations of the adaptive filtered-X least mean square (FXLMS) algorithm. Feedback controllers were designed using state space models obtained by fitting frequency domain data using the DynaMod software package. Both sets of controllers were implemented using two Innovative Integration SBC32 4-input/4-output boards. These boards contain Texas Instruments TMS320C32 Digital Signal Processors (DSPs) running at 60 MHz.

3.2 Feedforward Control--Introduction

Several controllers that were implemented on the testbed used an adaptive feedforward algorithm, Filtered-X Least Mean Square (FXLMS). Adaptive feedforward controllers using both the FSM actuator and control speaker were implemented separately. In the FXLMS algorithm, a reference sensor that is correlated with the disturbance input is filtered with an adaptive weight vector to produce an actuator drive signal. The filter weights are adapted based on an error measurement. The distinguishing feature of the FXLMS is that a model of the path from the control actuator to the error sensor is used in the adaptation of the filter weights. The advantage of the FXLMS algorithm over the strictly LMS algorithm is that the extra model allows broadband control of the incoming disturbance. Another variant of the FXLMS is the FXLMS with feedback neutralization (FXLMS-FN). In FXLMS-FN, a model of the control actuator to reference sensor transfer function is used to eliminate potentially destabilizing feedback.

Actual implementation of both the FXLMS and FXLMS-FN algorithms is a two-stage process. In the first stage, the identification stage, the control actuator is driven with random noise and the appropriate sensor signals measured. An LMS algorithm is used to fit FIR filters to the response from the actuator to the sensors. After these FIR filters have converged, the next stage is entered, actual implementation of the FXLMS algorithm. In theory and in practice, it is not important whether the disturbance is on or off during the identification stage as the LMS algorithm only fits the model to that part of the signal that is correlated with the input random noise.

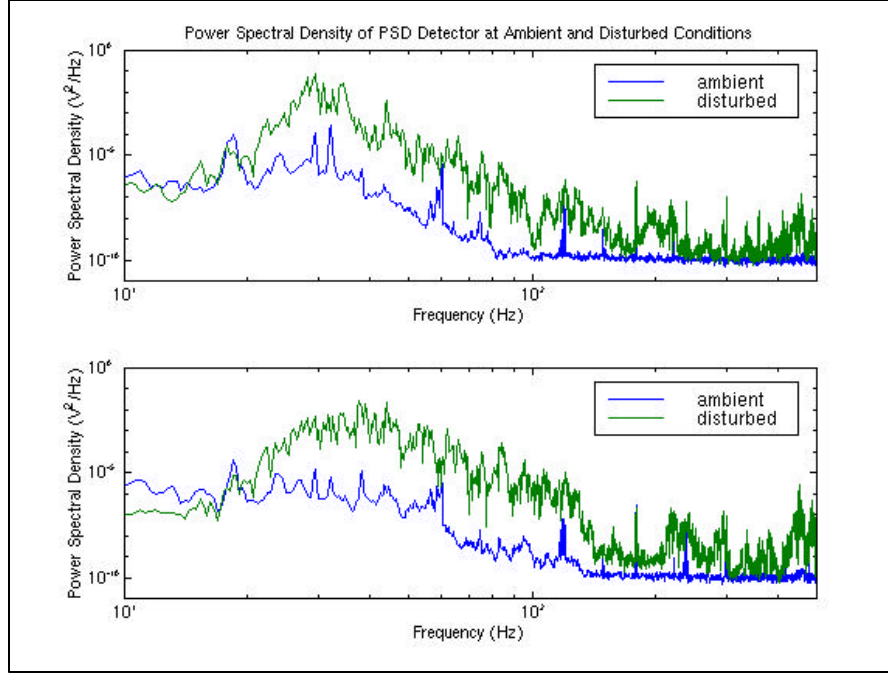


Figure 5: Comparison of ambient and disturbed power spectral densities for two axes of position sensing detector

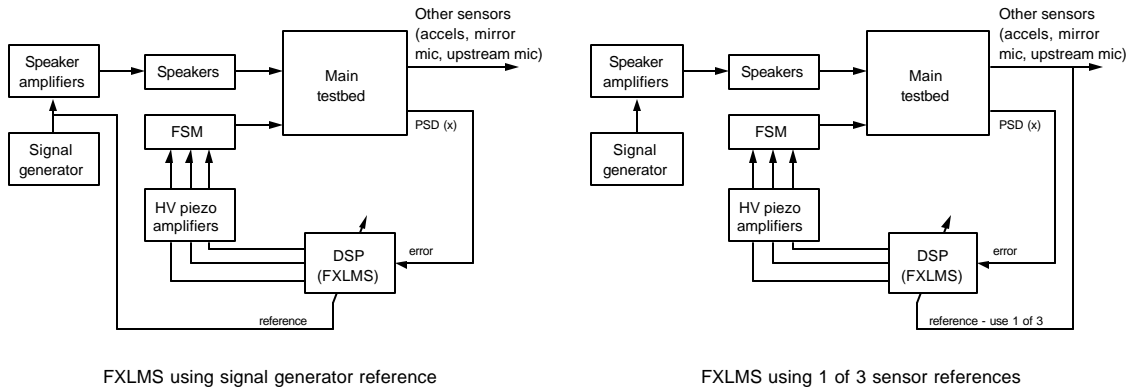


Figure 6: Architecture used in feedforward experiments

3.3 Feedforward Control Using Fast Steering Mirror

In feedforward control using the FSM, the only possible error sensor is the position sensing detector, because the FSM acts by steering the laser beam rather than producing mechanical or acoustic vibrations. Thus, the only difference in possible FSM topologies is the choice of reference sensors, of which there are several (Figure 10). The simplest and least realistic is to use the drive signal for the disturbance speakers as the reference sensor. More realistic choices for reference sensor are:

- microphone in disturbance enclosure
- microphone on mirror
- accelerometer on mirror

Each of these topologies was implemented for both a narrowband disturbance at 80 Hz and a broadband disturbance. 80 Hz was chosen as the narrowband disturbance frequency because the position sensing detector output exhibited a high response to the acoustic disturbance at this frequency. Table 1 shows a summary of the narrowband performance improvement for the different reference sensors with the x-axis position sensing detector as the error sensor. Note that all the reference sensors yield significant improvements in the jitter, but that some improvements are larger than others. In fact, the largest performance improvement is not using the signal generator as might be expected, but rather, uses the accelerometer mounted on the mirror. This is most likely because the acceleration of the mirror is more closely related to the jitter than the acoustic field. Additionally, note that the performance using the accelerometer and the microphone in the disturbance enclosure are both better than the performance using the signal generator. One possible explanation for this is that the accelerometer and microphone are able to detect disturbances at 80 Hz that are not caused by the speakers. Thus, the coherence between the error and the accelerometer or microphone is higher at the frequency of interest than the coherence between the signal generator and the error. Since the coherence between the error and the feedforward sensor determines the limit of performance, the performance is higher for the accelerometer and microphone. The acoustic field generates a displacement of the mirror, which is observed as jitter. The reason that the microphone on the mirror had the smallest performance improvement is that the correlation between the microphone and jitter measurements is lower than expected and is lower than the other sensors. This result does not bode well for jitter control using the acoustic actuator.

Table 1: Performance for FSM feedforward control of position sensing detector x-axis

Reference Sensor	Error Sensor	PSD Narrowband Performance (dB)	PSD Broadband Performance (dB)
1. Signal generator	PSD	-34.3	-9.5
2. Microphone on mirror	PSD	-32.0	-5.6
3. Microphone in disturbance enclosure	PSD	-44.5	-5.4
4. Accelerometer on mirror	PSD	-47.0	-7.4

Table 1 also shows the broadband performance from 0 to 1000 Hz. These broadband results were obtained with a FXLMS implementation using a 1200-tap FIR filter running at 2000 Hz. This yields an impulse response length of 600 ms. Although this high number of taps was very computationally demanding, it was required for good broadband performance. In contrast to the narrowband case, the best broadband performance was obtained using the function generator as the reference signal. This is most likely because the function generator provides a much flatter spectrum, which forces the adaptive filter to converge over all frequencies at an equal rate. The microphones and the accelerometers had a much more dynamic power spectrum, which forces the filter to converge at different rates at different frequencies. Due to finite precision effects, the adaptation will stop at frequencies with low energy in the reference signal, i.e., it will “lock up” before their optimum value is reached. However, the performance using the accelerometer was nearly as good as the performance using the signal generator. The broadband reduction of 7.4 dB is within the project goal of 5-8 dB.

3.4 Feedforward Control Using Acoustic Actuator

When using the control speaker, rather than the FSM, in a FXLMS feedforward algorithm, there is only one realistic choice for reference sensor, a microphone in the disturbance enclosure. The signal generator is also an option, but is not realistic for many situations, since one would almost never have this signal available in an uncorrupted sense in a real acoustic noise control problem. Exceptions to this are cases where a drive signal is required to operate a piece of equipment, such as cryocoolers and certain types of pumps. Both reference sensors were examined, but since they yielded similar results, only the case with the microphone as the reference sensor will be discussed. In the speaker case, there are a variety of possible error sensors

- microphone mounted on edge of mirror
- accelerometer mounted on mirror housing
- position sensing detector

Each of these topologies was examined for reduction in the error signal and improvement of the real performance, the position sensing detector output. In the speaker case with the microphone in the disturbance enclosure as the reference sensor, because the actuator and reference sensor are both acoustic transducers, there is the possibility for feedback from the control actuator to the reference sensor. This feedback can lead to instability of the FXLMS algorithm unless feedback neutralization (FXLMS-FN) is employed. In FXLMS-FN, an estimate of the feedback from the control actuator to the

reference sensor is subtracted from the actual reference sensor measurement and this new value is used to compute the actuator output.

Only narrowband experiments were performed using the control speaker. The narrowband experiments again used the 80 Hz disturbance input. Table 2 summarizes the narrowband results for the different error sensors with a microphone in the disturbance enclosure as the reference sensor. Note that for each error sensor, there is significant performance improvement at the error sensor, but that performance does not necessarily translate into good performance at the position sensing detector. In the case of the microphone error sensor, closing the loop actually made the position sensing detector performance worse and for the accelerometer error sensor, the position sensing detector measurement was reduced by only 5.8 dB broadband. The fact that using the position sensing detector itself as the error sensor results in such high performance indicates that the acoustic actuator can reduce the measured jitter, but raises the question of what the exact mechanism of the reduction is.

Table 2: Performance for error sensors and position sensing detector for narrowband FXLMS-FN using acoustic actuator

Reference Sensor	Error Sensor	Error Sensor Performance (dB)	Position Sensing Detector Performance (dB)
Microphone upstream	Mirror microphone	-22.4	+1.4
Microphone upstream	Mirror accelerometer	-19.4	-5.8
Microphone upstream	Position sensing detector single axis	-28.4	-28.4

If it is assumed that the testbed is perfect and the only source of jitter is the mirror vibrating on its flexures excited by the impinging acoustic field, then it seems obvious that a reduction in the vibration of the mirror as measured by the accelerometer would translate directly into an equal jitter reduction in the measurement of the position sensing detector. It can be argued that reduction of the pressure at a single point near the mirror will not produce large jitter reductions because the pressure field may still be large elsewhere on the mirror. This fact suggests that a better acoustic error signal would be some combination of an array of microphones around the mirror.

Since the accelerometer reduction did not result in large jitter reduction, it can be surmised that there must be other sources of jitter, flanking paths, in the testbed. The flanking paths are mechanical vibration paths that excite the optics bench and the ceiling beam upon which the position sensing detector is mounted. The presence of these paths could be heard and felt by listening to the ceiling vibrate in other parts of the building and feeling the vibrations in the optics bench. Distinguishing between the primary path and the flanking paths for jitter is impossible with the current testbed set up. To determine the jitter component due to the acoustic field impinging on the mirror, additional sensors are required.

Another fact to consider is that the control speaker is not solely an acoustic actuator, but is also a reaction mass actuator. Thus, driving the control speaker not only generates acoustic waves but also mechanical vibration waves in the testbed. Thus, it is unclear which aspect of the control actuator is dominant in reducing the jitter in the position sensing detector error sensor case. It seems more likely that the reaction mass actuator aspect, rather than the acoustic actuator aspect, is being used to set up canceling vibrations either on the optics bench or at the ceiling beam. This hypothesis is partially confirmed by using a bass shaker to control the jitter. The bass shaker produces mechanical vibrations without producing acoustic waves. Jitter performance using the bass shaker is of a similar level as for the speaker indicating that the jitter in the testbed can be controlled using a purely mechanical actuator, rather than the combined mechanical and acoustic actuation of the speaker.

3.5 Feedback Control Using Acoustic Actuator

The first feedback controllers were implemented using the acoustic actuator within the square optics enclosure. These controllers were designed using a 109 state, 2 input, and 7 output model that matched the data fairly well. Linear Quadratic Gaussian (LQG) feedback controllers were designed using microphones, accelerometers, or a combination to minimize the measured jitter. Three of the topologies examined (A through C) are discussed in Table 3.

It was decided that the control designs using these topologies were to be limited to stable controllers. While there is nothing inherently bad with unstable controllers, extreme care must be exercised in their implementation. Figure 7 shows the power spectral density performance plots for the two position sensing detector axes for topology A as implemented on the testbed. It is noted that there is not a large change from open to closed-loop, but that there is some performance improvement in the 50 to 60 Hz range and at approximately 25 Hz in the upper plot. Also note that there is amplification at some frequencies. Performing a backsum on the power spectral densities to determine the RMS levels reveals that the implementation of control

actually increased the jitter by 20%. It should be kept in mind, however, that the performance objective for this topology was the microphone located at the mirror. Thus, looking that these power spectral densities is not a fair comparison. Rather, the acoustic levels at the microphone should be examined. Figure 8 shows the transfer function from the disturbance speakers to the mirror microphone for the open and closed-loop cases. Note that the most performance is achieved at the mode at approximately 40 Hz. This isn't surprising, since because of the bandwidth limit imposed by the compensator stability constraint, the control to feedback transfer function has its largest magnitude, and consequently largest control authority, in this region. This 40 Hz mode roughly corresponds to the first closed end-open end tube mode for the beam tube and the actuator modes of the speakers. Thus, the controller cancels the effects of the first acoustic mode on the mirror microphone.

Table 3: Summary of feedback topologies

Case	Actuator	Error Sensor	Performance quantities
A	Speaker	microphone on mirror	microphone on mirror
B	Speaker	two accels. on mirror, microphone on mirror, microphone upstream in beam tube	two axes of PSD, two accels. on mirror, microphone on mirror
C	Speaker	microphone on mirror, two mics upstream in beam tube	two axes of PSD, microphone on mirror
D	Fast steering mirror (FSM)	two axes of PSD	two axes of PSD

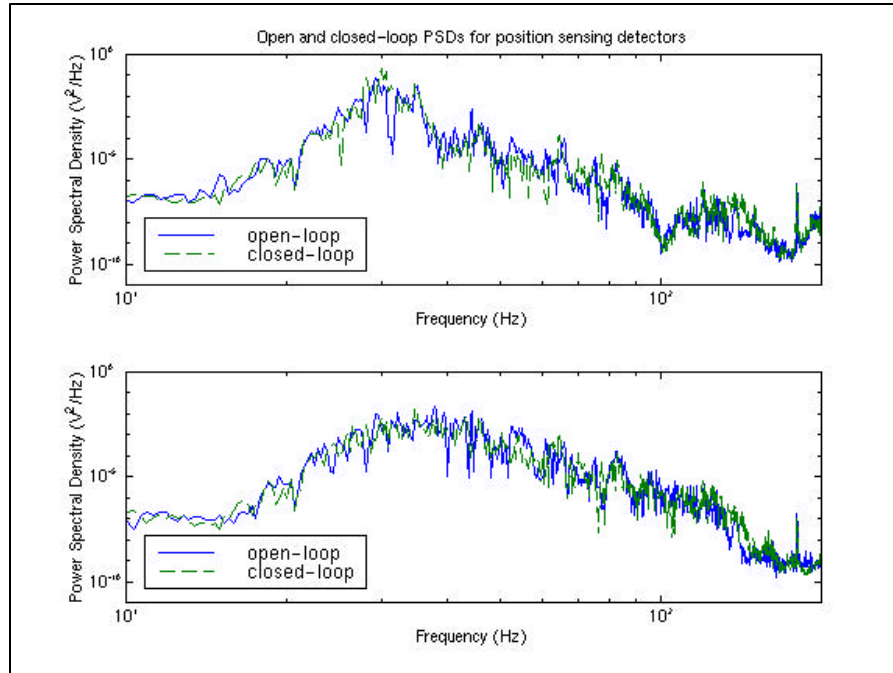


Figure 7: Open and closed-loop power spectral densities for position sensing detector for acoustic actuator feedback controller (Topology A)

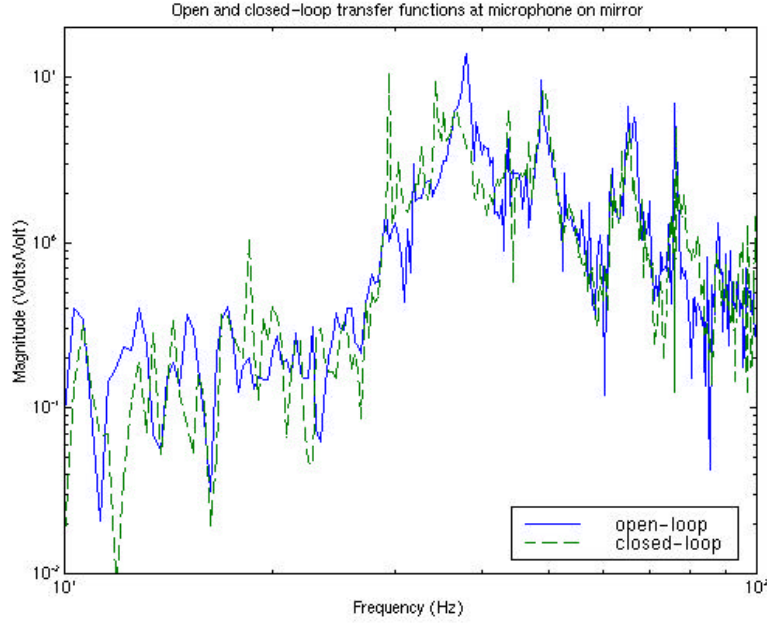


Figure 8: Disturbance to mirror microphone transfer function, open and closed-loop, using acoustic actuator, feedback controller

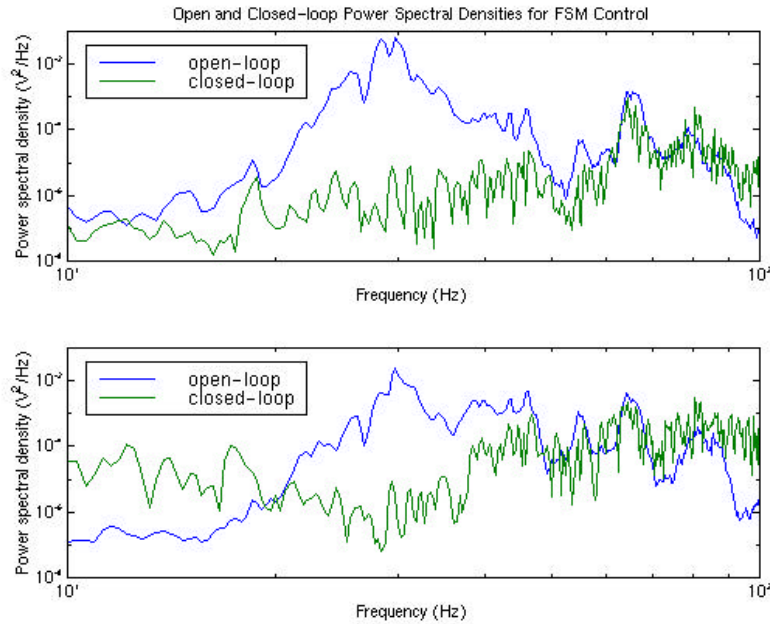


Figure 9: Open and closed-loop power spectral densities for position sensing detectors with FSM control

3.6 Feedback Control Using Fast Steering Mirror

The second set of feedback control results used the fast steering mirror as the actuator and the position sensing detector as the feedback and performance sensors (topology D in Table 3). A FSM consists of three piezoelectric stack actuators arranged in a circular pattern separated by 120 degrees. Thus, by a proper combination of the FSM leg inputs, the FSM can be actuated in piston, tip, and tilt modes. A mixing matrix for the three FSM leg inputs was constructed such that FSM tip and tilt motions were aligned with the position sensing detector axes. This mixing matrix was incorporated in a 16 state two-input/two-output state space model and used to design LQG controllers. Since the open-loop power spectral densities of the position sensing detector have a significant response near 30 Hz, frequency weights targeting this region were included in the

control design. The result is a control law that is highly effective at 30 Hz. Figure 9 shows the open and closed-loop power spectral densities for this two-axis FSM controller with a notch at 30 Hz. Note that the high responses near 30Hz have been completely eliminated in the closed-loop case. Performance is far superior to that achieved with the acoustic actuator (topologies A, B, and C in Table 3). This type of control is exactly the type of optical servo control that will be implemented on the real ABL system.

3.7 Combined FSM Feedback and Acoustic Feedforward Control

The last set of control results utilizes a combination of FSM feedback control and adaptive FXLMS feedforward control using the acoustic actuator. These two controllers were run independently on separate SBC32 DSP boards, with the 30 state FSM controller running at 12 kHz and the 48 tap acoustic FXLMS-FN running at 5 kHz. The intent of these control experiments was to better replicate the actual ABL situation compared to what had been done using only the FSM or the acoustic actuator. In the ABL, optical servo loops around the FSM and tip-tilt sensors would be closed to reject both vibration and acoustic disturbances. These optical servo loops would have limited bandwidth. Any disturbances above the bandwidth would not be rejected. In the ABL, there are several pieces of rotating machinery, such as the basic hydrogen peroxide (BHP) turbopump. Often, rotating machinery produces noise at discrete tones related to the spin speed and harmonics. If these tones lie outside the bandwidth of the optical servo loops, they can cause significant jitter. The acoustic jitter reduction controllers can be used to reduce these unwanted tones. By using an independent actuator, the potential instability associated with two controllers operating independently can largely be avoided.

In this set of experiments, the acoustic disturbance is set to be a superposition of broadband noise with a single tone at 80 Hz. First, the previously discussed two-axis FSM controller is implemented, followed by one of several acoustic FXLMS-FN loops using various error sensors. Three error sensors were examined:

- microphone mounted on edge of mirror
- accelerometer mounted on mirror housing
- one axis of the position sensing detector

Figure 10 shows the open and closed-loop autospectra for the position sensing detector y-axis with the FSM and acoustic feedforward controllers operating. Note that except for the 80 Hz range all the closed-loop results lie on top of one another, indicating that the FSM feedback controller and the acoustic feedforward controllers are operating without any detrimental effects. Note that the FSM control amplified the jitter response above 100 Hz, which can be alleviated somewhat with a better FSM control design.

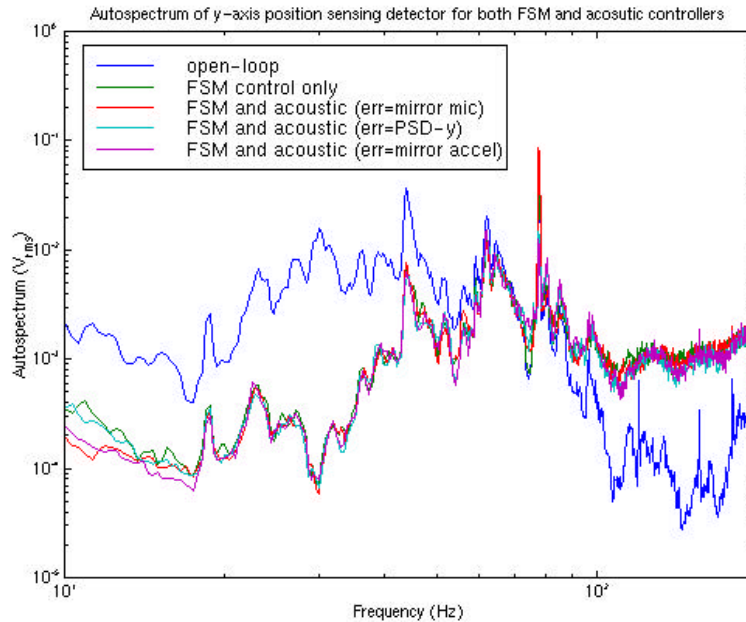


Figure 10: Open and closed-loop autospectra of position sensing detector y-axis for FSM and acoustic controllers (feedback plus feedforward)

It was interesting to note that even though the disturbance was broadband in nature with a tone superimposed, the feedforward acoustic control still operated as if it were controlling a single tone. Figure 11 shows a close up of the 80 Hz tonal response, showing the effects of the acoustic feedforward control, which achieved an extra 10 dB of narrowband jitter performance at the 80 Hz tone over and above the optical servo loops. Note that the same general trends across different error sensors are seen in the fully coupled control as were seen in the individual acoustic control.

This last set of control results is significant because it replicates, to a high degree, the situation present in the actual ABL, namely optical servo loops operating in the presence of acoustic disturbances. The residual effects of the acoustic disturbances on the optical jitter are then reduced using a separate acoustic actuator and control system. This is attractive because the addition of an extra layer of FSM control and the necessary software modifications it entails makes introduction of the technology a remote possibility. Furthermore, the fact that the acoustic controller operates without degrading the optical servo loops is significant because it shows that adding the extra acoustic control loop only enhances the closed-loop jitter performance. These control results prove the feasibility of the active acoustic jitter suppression concept.

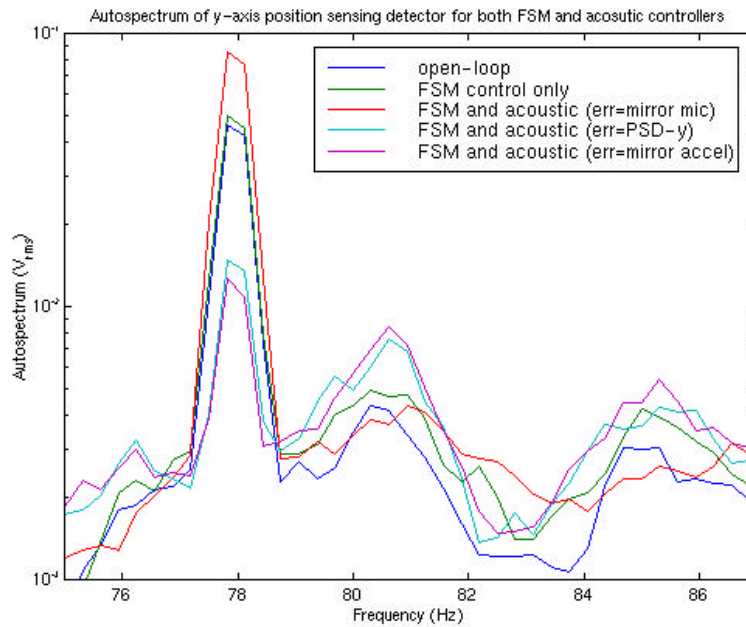


Figure 11: Close up of autospectra at 80 Hz

3.8 Combined FSM Feedback and Feedforward Control

This last topology utilizes a combination of FSM feedback control and adaptive FXLMS feedforward control also using the FSM. These two controllers were run simultaneously on a single SBC32 DSP board. Because of the extra computations imposed by the addition of the feedforward control, the previous 30 state two-axis FSM feedback control running at 12 kHz using the position sensing detector could not be used. Instead, a single axis 23 state FSM controller was designed to be run at 2 kHz. The same design methodology as for the previous controller was again used for this new controller at a slower sampling rate. Simultaneously with the feedback controller, a 64 tap FXLMS controller was also running. The error sensor for the FXLMS and the feedback sensor were both set to be the appropriate axis of the position sensing detector. The reference sensor for the FXLMS was a microphone inside the disturbance enclosure, but outside the beam tube. The control outputs of the two controllers were then summed to give the output that was sent to the FSM legs via the D/A converters.

The intent of these control experiments was to attempt to determine the extent to which the two controllers would interact while controlling the same actuator. It is expected that the FSM feedforward approach will achieve the best performance, because the performance metric (jitter as measured by the position sensing detector) is controlled directly with the FSM. Thus, these control results are important because an interaction between the feedback and feedforward controllers that results in instability will mean that this topology would be eliminated from further contention. In this set of experiments, the acoustic disturbance is again set to be the superposition of broadband noise with a single tone at 80 Hz.

Figure 12 shows the open and closed-loop autospectra for the position sensing detector y-axis with the FSM feedback and feedforward controllers operating. Note that except for the 80 Hz range, both sets of closed-loop results are very similar, indicating that the FSM feedback controller and the feedforward controllers are operating without any serious detrimental effects.

It was interesting to note that as for the FSM feedback-acoustic feedforward topology, even though the disturbance was broadband in nature with a tone superimposed, the feedforward control still operated as if it were controlling only a single tone. Figure 13 shows a close up of the 80 Hz tonal response, showing the effects of the feedforward control, which achieved nearly an extra 20 dB of narrowband jitter performance at the 80 Hz tone over and above the optical servo loop.

This last set of control results is significant because it shows the two layers of control do not destabilize each other and that adding the extra FSM feedforward control loop only enhances the closed-loop jitter performance. With the completion of this last set of control results, the feasibility of the concept has been proved experimentally.

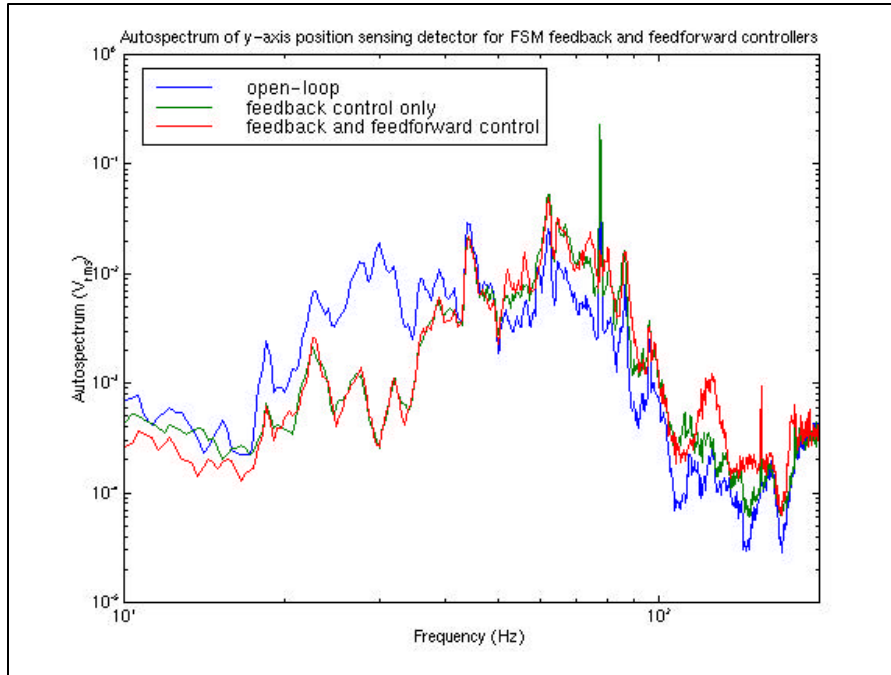


Figure 12: Open and closed-loop autospectra of position sensing detector y-axis for FSM controllers (feedback plus feedforward)

4. CONCLUSIONS

This paper summarizes the results of a Phase I Small Business Innovation Research program. The Phase I effort focused primarily on development of a testbed that captured the fundamental physical behavior of the Airborne Laser acoustically induced jitter problem and demonstrating different active control topologies for reducing the effects of acoustic disturbances on optical jitter. Two actuators were used for control, a fast steering mirror and a secondary speaker. Several different sensor types, microphones, accelerometers, and optical position sensing detector were used with these two actuators in both adaptive feedforward and fixed feedback control formulations.

Narrowband control at 80 Hz using an adaptive feedforward algorithm with the fast steering mirror as the actuator, an accelerometer on the mirror as the reference sensor, and the position sensing detector as the error sensor achieved 47.0 dB of narrowband jitter reduction. Broadband control using an accelerometer as the reference signal and the position sensing detector as the error sensor achieved 7.4 dB of reduction from 0 to 1000 Hz. Narrowband control at 80 Hz using an adaptive feedforward algorithm with a secondary speaker as the actuator, a microphone inside the disturbance enclosure as the reference sensor, and the position sensing detector as the error sensor achieved 28.4 dB narrowband performance improvement at the 80 Hz tone. These results indicate that significant narrowband jitter reduction can be achieved using either actuator topology.

Feedback control using a secondary speaker in the optical enclosure to reduce the acoustic field measured by microphones mounted on the mirror achieved good broadband acoustic reductions. These acoustic reductions did not, however, translate into good jitter reduction as measured by the position sensing detector. This indicates that the measured jitter is a

combination of acoustically induced jitter on the mirror and vibration induced jitter on the metrology system and mirror. Feedback control using the fast steering mirror as the actuator and the position sensing detector as the feedback sensor achieved good broadband reduction in the measured jitter. This type of control topology is the type that would be baselined into the ABL architecture as low level optical servo loops.

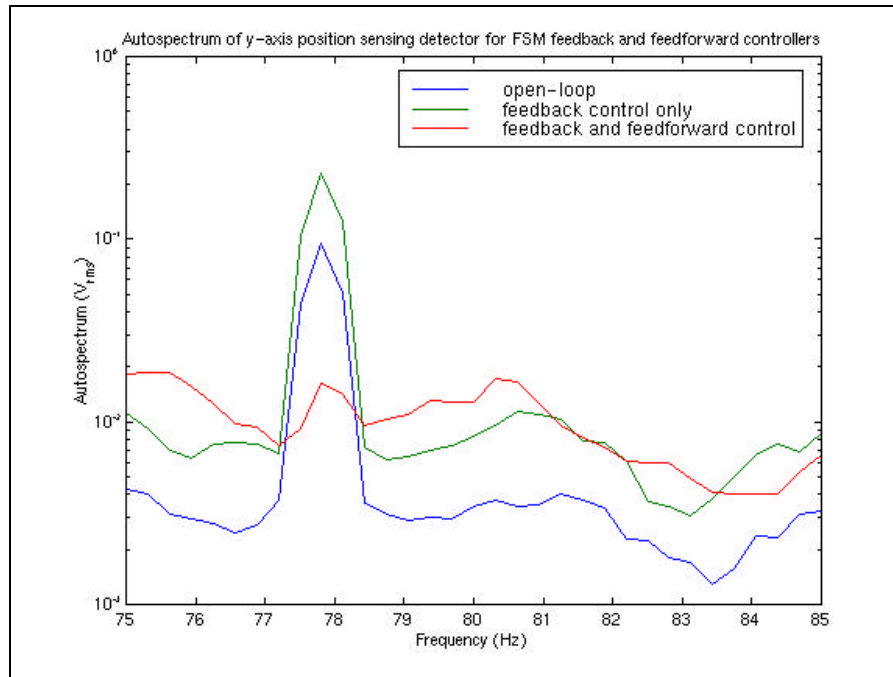


Figure 13: Close up of autospectra at 80 Hz

Hybrid topologies using a combination of fast steering mirror feedback control and feedforward control using either the fast steering mirror or the secondary speaker were implemented. These hybrid topologies were used to reduce the jitter caused by a broadband disturbance superimposed with a narrowband tonal input at 80 Hz. The FSM feedback control provided the broadband control and the feedforward control reduced the tonal disturbance. Furthermore, the fact that the two independent controllers were implemented simultaneously shows that there is not a destabilizing interaction between the two. The most important conclusion of this effort is that this experimental result implies that the additional controller commands required to implement FSM feedforward control in the real ABL system can be safely added to the baseline control commands without causing instability.

ACKNOWLEDGEMENTS

This work was performed under a Phase I Small Business Innovation Research funded by the Air Force Research Laboratory under Contract F04701-98-C-0103, with Dr. Steven Griffin serving as technical monitor. The authors gratefully acknowledge Lockheed Martin for the loan of optical equipment, and Dr. Paul Merritt and Dr. Bruce DeShetler of SVS R&D, Inc. for their insights into jitter control for precision optical systems.

REFERENCES

1. Widrow, B. and Stearns, S., 1985, *Adaptive Signal Processing*, Prentice Hall, Inc., Englewood Cliffs, NJ.
2. Kuo, S. and Morgan, D., 1996, *Active Noise Control Systems*, John Wiley and Sons, New York.